0026-895X/09/7505-1117–1126$20.00
MOLECULAR PHARMACOLOGY
Copyright © 2009 The American Society for Pharmacology and Experimental Therapeutics
Mol Pharmacol 75:1117–1126, 2009

Vol. 75, No. 5
52209/3465517
Printed in U.S.A.

Mrp1 Localization and Function in Cardiac Mitochondria after Doxorubicin

Paiboon Jungsuwadee, Ramaneeya Nithipongvanitch, Yumin Chen, Terry D. Oberley, D. Allan Butterfield, Daret K. St. Clair, and Mary Vore

Graduate Center for Toxicology (P.J., Y.C., D.K.S., M.V.), and Department of Chemistry and Center of Membrane Sciences (D.A.B.), University of Kentucky, Lexington, Kentucky; and Department of Pathology and Laboratory Medicine, University of Wisconsin Medical School, Madison, Wisconsin, (R.N., T.D.O.)

Received September 22, 2008; accepted February 18, 2009

ABSTRACT

Multidrug resistance-associated protein 1 (Mrp1; Abcc1) is expressed in sarcolemma of murine heart, where it probably protects the cardiomyocyte by mediating efflux of endo- and xenobiotics. We used doxorubicin (DOX), a chemotherapeutic drug known to induce oxidative stress and thereby cardiac injury, as a model cardiotoxic compound and observed changes in the Mrp1 expression pattern in cardiac tissue of DOX- versus saline-treated mice. Confocal immunofluorescent and immunogold electron microscopy, together with subcellular fractionation followed by immunoblot analyses and transport measurements, localized functional Mrp1 to mitochondria after DOX. Expressions of Mrp1 in heart homogenate, sarcolemma, and submitochondrial particles (SMP) were increased 1.6-, 2-, and 3-fold, respectively, at 24 h after DOX. Mitochondrial Mrp1 expression was markedly increased 72 h after DOX, whereas transport of Mrp1 substrates in SMP was maximal at 24 h. ATP-dependent transport in SMP occurred into an osmotically sensitive space and was inhibited by the anti-MRP1 antibody QCRL3. Adduction of a 190-kDa protein with the reactive lipid peroxidation product 4-hydroxy-2-nonenal (HNE) was detected in SMP and was maximal at 72 h after DOX; immunoprecipitation confirmed Mrp1-HNE adduction. In vitro, HNE (10 μM) inhibited mitochondrial respiration and transport activity in SMP, suggesting that Mrp1 is adversely affected by oxidative stress. These data demonstrate that after DOX, functional Mrp1 is detected in mitochondria in addition to that in sarcolemma; however, adduction with HNE inhibits Mrp1 activity. Mrp1 may serve to protect the heart by mediating the efflux of toxic products of oxidative stress from mitochondria and cardiomyocytes.

Cardiomyopathy is a serious, dose-dependent toxicity associated with doxorubicin (DOX) use in cancer chemotherapy (Singal and Iliskovic, 1998). DOX is proposed to induce cardiotoxicity because of its ability to generate reactive oxygen species via quinone redox cycling (Gille and Nohl, 1997). In mice, DOX treatment enhances the production of the highly reactive lipid peroxidation product 4-hydroxy-2-nonenal (HNE) in cardiac tissue, decreases mitochondrial membrane fluidity, and causes mitochondrial dysfunction (Zhou et al., 2001; Chaiswing et al., 2004). Based on the relative redox states, mitochondria are the most reducing subcellular organelle (Hansen et al., 2006), thereby making mitochondria the most vulnerable target of oxidation in an oxidative milieu. Given the heart's high oxygen consumption (8 ml of O_2/min per 100 g), its high mitochondrial content (40% of noncollagenous protein) (Mela-Riker and Bukoski, 1985), and mitochondria as the major site of oxygen utilization (80%) (Jain and Fischer, 1989), damage to cardiac mitochondria is considered a major contributor to DOX-induced cardiomyopathy. However, the causative factors involved in the mitochondrial dysfunction remain unclear.

Multidrug resistant-associated protein 1 (MRP1/ABCC1) is a member of the ATP-binding cassette (ABC) transporter protein superfamily, subfamily C (Cole et al., 1992). Mrp1 is ubiquitously expressed in several tissues, including heart (Flens et al., 1996), where it localizes in sarcolemma mem-

This work was supported by the National Institutes of Health National Cancer Institute [Grants CA94853, CA139844] and the National Institutes of Health National Institute of General Medical Sciences [Grant GM55343].

Article, publication date, and citation information can be found at http://molpharm.aspetjournals.org.

doi:10.1124/mol.108.052209.

ABBREVIATIONS: DOX, doxorubicin; $E_2$17G, estradiol 17β-D-glucuronide; GAPDH, glyceraldehyde-3-phosphate dehydrogenase; GSTα, glutathione transferase α; HEK, human embryonic kidney; HEK_{Mrp1}, pCEBV7-Mrp1-transfected human embryonic kidney 293 cells; HNE, 4-hydroxy-2-*trans*-nonenal; LAMP2, lysosome-associated membrane protein 2; Mrp1, murine multidrug resistant-associated protein 1; SDHB, succinate dehydrogenase subunit B; SMP, submitochondrial particles; VDAC, voltage-dependent anion channel; ABC, ATP-binding cassette; LTC_4, leukotriene C_4; mAb, monoclonal antibody; TBS, Tris-buffered saline; DMSO, dimethyl sulfoxide; GS-HNE, glutathione conjugate of 4-hydroxy-2-*trans*-nonenal; Na^+/K^+-$ATPase_{\alpha 1}$, anti-sodium/potassium-ATPase α1; pAb, polyclonal antibody.

brane (Jungsuwadee et al., 2006). Its localization in plasma membrane has led to the concept that Mrp1-mediated efflux of substrates from cells serves a protective role. In addition to effluxing certain chemotherapeutic drugs, MRP1 plays a significant role in transporting glutathione and glucuronide conjugates, such as leukotriene C_4 (LTC_4) and estradiol-17β-D-glucuronide ($E_2$17G) (Deeley and Cole, 2006). DOX-induced HNE production is partially detoxified by conjugation with GSH by glutathione transferase (GST) to form the glutathione conjugate of HNE (GS-HNE) (Alin et al., 1985), also an MRP1 substrate (Renes et al., 2000). Perfusion of the rat heart with HNE leads to the formation and saturable efflux of GS-HNE (Srivastava et al., 1998), suggesting a role for MRP1 in the clearance of GS-HNE from cardiac tissue. These data led us to conclude (Jungsuwadee et al., 2006) that Mrp1 probably mediates the saturable efflux of the glutathione conjugate of HNE observed upon infusion of HNE to the perfused heart (Ishikawa et al., 1986) and thereby serves to protect the cardiomyocyte.

Here we further investigated the expression and localization of Mrp1 in mice treated with DOX and found that although Mrp1 was localized primarily in sarcolemma in control heart (Jungsuwadee et al., 2006), significant functional Mrp1 was also detected in heart mitochondria after DOX treatment. However, DOX treatment also increased HNE adduction of mitochondrial Mrp1 and decreased its function.

Materials and Methods

Reagents. [^{3}H]$E_2$17G (39.8 Ci/mmol), [^{3}H]LTC_4 (160 Ci/mmol), and [^{3}H]GSH ([glycine-2-^{3}H]; 41.5 Ci/mmol) were purchased from PerkinElmer Life and Analytical Sciences (Waltham, MA). Doxorubicin HCl was from Bedford Laboratories (Bedford, OH), MRP1 monoclonal antibodies (MRPr1 and QCRL3 mAb) were from Alexis (San Diego, CA), mouse anti-sodium/potassium-ATPase α1 (Na^+/K^+-$ATPase_{\alpha1}$) mAb from Millipore Corporation (Billerica, MA), rat anti-lysosome-associated membrane protein 2 (LAMP2) mAb was from Abcam (Cambridge, MA), and rabbit anti-HNE-Michael adducts polyclonal antibody and mouse anti-voltage-dependent anion channel (VDAC) mAb were from Calbiochem (San Diego, CA). Rabbit anti-rat GST α pAb was from (Biotrin, Dublin, Ireland), Alexa Fluor 488 was from Invitrogen (Carlsbad, CA), donkey anti-rabbit Cy3 was from Jackson ImmunoResearch Laboratories (West Grove, PA), and rabbit anti-succinate dehydrogenase subunit B (SDHB) pAb, rabbit anti-glyceraldehyde-3-phosphate dehydrogenase (GAPDH) pAbs, and Protein A/G agarose beads were from Santa Cruz Biotechnology (Santa Cruz, CA). Purified mouse IgG2a was purchased from BD Biosciences (San Jose, CA). Anti-rat Ig-, anti-rabbit Ig-, and anti-mouse Ig-horseradish peroxidase and ECL Plus were obtained from GE Healthcare (Chalfont St. Giles, Buckinghamshire, UK).

Animals. C57BL/6 (The Jackson Laboratory, Bar Harbor, ME), FVB, and Mrp1-disrupted FVB [Mrp1(−/−); Taconic Transgenics, Hudson, NY] mice were maintained in the Division of Laboratory Animal Resources facility and were provided food and water ad libitum. All experiments complied with the requirements of the Institutional Animal Care and Use Committee of the University of Kentucky. Mice were treated intraperitoneally with normal saline solution (saline) or 20 mg/kg DOX, and the heart was removed at various times thereafter, as indicated in the figure legends. The rationale for the dose of 20 mg/kg DOX used here is its equivalency in mice to that used to treat small cell lung cancer (Piscitelli et al., 1993), together with the ability of this dose to induce reproducible cardiac injury in C57BL/6 mice (Freireich et al., 1966; Chabner et al., 2001).

Isolation of Submitochondrial Particles and Sarcolemma Membrane. Hearts were homogenized in buffer A (0.225 M mannitol, 0.075 M sucrose, 1 mM EGTA, and protease inhibitors 1 mM phenylmethylsulfonyl fluoride, 1 μg/ml leupeptin, 1 μg/ml aprotinin, and 1 μg/ml pepstatin), centrifuged at 480*g* for 5 min, and the pellet (fraction B) was used to isolate sarcolemma as described previously (Jungsuwadee et al., 2006). The supernatant (fraction A) was filtered through a double layer of cheese cloth followed by centrifugation at 7700*g* for 10 min. The mitochondrial pellet was washed, resuspended in buffer A, and stored at −20°C for ≥16 h. The mitochondrial pellets were thawed, resuspended in submitochondrial particle (SMP) buffer (250 mM sucrose, 15 mM $MgCl_2$, and 1 mM ATP) (Linnane and Ziegler, 1958), followed by sonication (5% output, 550 Sonic Dismembrator) for 30 s, and subsequently centrifuged at 15,800*g* for 8 min. SMP pellets were resuspended in TS buffer (10 mM Tris HCl and 250 mM sucrose, pH 7.4) and centrifuged at 100,000*g* for 40 min at 4°C. To further purify the SMP pellets, they were resuspended in TS buffer, overlaid on 38% sucrose, and centrifuged at 9300*g*, for 10 min at 4°C. The purified SMP pellet was resuspended in TS buffer, and protein concentration was determined using the BCA protein assay (Jungsuwadee et al., 2006). Plasma membranes from HEK293 cells stably transfected with Mrp1 (HEK_{Mrp1}) were prepared as described previously (Jungsuwadee et al., 2006).

Synthesis and Purification of GS-HNE. The [^{3}H]GSH-conjugate of HNE ([^{3}H]GS-HNE) was formed by incubation of a 10-fold molar excess of HNE with [^{3}H]GSH in 100 mM Tris, pH 7.2, containing 2 units of rat liver GST (Renes et al., 2000). The reaction was performed at 37°C for 2 h or until the rate of loss of HNE remained unchanged as monitored by decreasing HNE absorbance at 224 nm. Unlabeled GS-HNE was generated by incubation of freshly prepared GSH with HNE in a 1:1 M ratio in the presence of 20 mM potassium phosphate buffer, pH 6.8, at 37°C with gentle mixing (Renes et al., 2000). The reaction mixtures were purified by high-performance liquid chromatography on a Symmetry C18, 4.6 × 250-mm column (Waters Corporation, Milford, MA) by using a linear gradient from 0 to 100% solvent B (0.05% trifluoroacetic acid in acetonitrile) in solvent A (0.05% trifluoroacetic acid in water) over 25 min at a flow rate of 1 ml/min. The column effluent was monitored at 210 nm, and peak fractions (retention time between 11 and 13 min) were collected, lyophilized, and redissolved in absolute ethanol. The concentration of GS-HNE was measured by a colorimetric assay (Renes et al., 2000).

Na^+/K^+-ATPase Activity Assay. The ATPase activity assay was performed as described previously (Jungsuwadee et al., 2006) using a coupled enzyme reaction to monitor oxidation of NADH in the presence and absence of ouabain.

Immunoprecipitation and Immunoblot Analysis. SMP protein was immunoprecipitated with anti-MRPr1 mAb as described previously (Jungsuwadee et al., 2006). Immunoprecipitated samples fractionated by 4 to 12% Tris-glycine SDS-polyacrylamide gel electrophoresis (Invitrogen, Carlsbad, CA) were analyzed by immunoblot for HNE-Michael adducts. Membrane fractions were subjected to immunoblot analysis; blots were probed with antibodies for Mrp1 (1:1000), HNE-Michael adducts (1:500), Na^+/K^+-$ATPase_{\alpha1}$ (1:40,000), LAMP2 (1:5000), SDHB (1:10,000), glutathione transferase α (GSTα) (1:1000), VDAC (1:20,000), and GAPDH (1:5000).

Confocal Scanning Laser Microscopy. Samples of left ventricle were obtained from mice 24 and 72 h after treatment with saline or DOX, and cryosections were prepared as described previously (Jungsuwadee et al., 2006). Tissue sections were blocked with 2% bovine serum albumin in phosphate-buffered saline containing 0.03% Triton X-100 for 60 min and were incubated with primary antibody against Mrp1 (1:100) and SDHB (1:200) at 4°C overnight. Tissue sections were then washed and probed with secondary antibodies (1:200) at room temperature for 2 h in the dark. Tissue sections were washed, air-dried, mounting medium was added, and sections were placed under a cover glass. Images were taken as described previously (Jungsuwadee et al., 2006).

Immunogold Ultrastructural Analysis. Left ventricles were fixed, embedded, and processed for immunogold electron microscopy as described previously (Oberley, 2002) with minor modifications. Embedded tissue blocks from each mouse were sectioned and transferred to nickel grids. Grids were rinsed with TBS, blocked with acetylated bovine serum albumin, and then washed with phosphate-buffered saline. The grids were incubated with anti-MRPr1 mAb at 4°C overnight, washed with TBS, and incubated with gold-conjugated secondary antibody [15-nm gold-conjugated $F(ab')_2$ fragment of goat anti-rat IgG (BB International, Cardiff, UK) diluted 1:30] for 90 min at room temperature. Grids were then rinsed with TBS followed by double-distilled H_2O. Grids were counterstained with 7.7% uranyl acetate for 10 min and photographed with an electron microscope (Hitachi H-600) operated at 75 kV. Photographs of 30 cardiomyocytes at 8000× from saline and DOX-treated mice were taken from each group, and the area of mitochondria was outlined and measured by image analysis software (Scion Image Beta 4.02; Scion Corporation, Frederick, MD). Gold beads within mitochondria were counted for quantification of immunoreactive Mrp1. The mean density of gold beads per square micrometer was expressed as mean ± S.E.M. of 30 cardiomyocytes per group.

Transport Studies. The transport experiments were performed as described previously (Jungsuwadee et al., 2006). SMP vesicles were made by vesiculation through a 26-gauge needle 15 times and once more immediately before the transport assay. ATP-dependent transport of [^{3}H]$E_2$17G and [^{3}H]GS-HNE into SMP (10 μg of protein/20 μl) was measured in incubations at 37°C for 1 min or as indicated in the figure legends. ATP-dependent transport of [^{3}H]LTC_4 was measured at 23°C for 1 min, and reactions were filtered onto a membrane filter. Radioactivity collected on the filters was detected by liquid scintillation counting using scintillation counting cocktail (Bio-Safe II; Research Products International Corp., Mt. Prospect, IL) as described previously (Jungsuwadee et al., 2006).

Measurement of Mitochondrial Respiration. Cardiac mitochondria were isolated from mice 24 h after DOX treatment and resuspended in buffer containing 250 mM sucrose, 50 mM HEPES, 2 mM $MgCl_2$, 1 mM EGTA, 10 mM KH_2PO_4, and 0.5% bovine serum albumin. Oxygen consumption was measured using a Clark-type electrode oxygraph (Hansatech, Norfolk, UK) with 10 mM pyruvate and 5 mM malate as substrate in the absence of exogenous ADP (state 2 respiration) and after the addition of 300 mM ADP (state 3 respiration). Oligomycin, the ATPase inhibitor (100 μg/ml), was then added to inhibit mitochondrial state 4 respiration. In normally coupled mitochondria, the addition of oligomycin slows respiration to a rate similar to that of state 2, whereas in uncoupled mitochondria, oligomycin inhibition is reduced. The respiratory control ratio was calculated as the ratios between state 3 and state 4 respiration.

Statistical Analysis. Data of quantitative results were expressed as mean ± S.E.M. or as otherwise indicated. Statistical analyses were performed using one-way analysis of variance followed by a post hoc test on GraphPad Prism 4 (GraphPad Software Inc., San Diego, CA). A p value <0.05 was considered as a significant difference.

Results

Mrp1 Protein Expression in Mitochondria after DOX Treatment. Mrp1 is constitutively expressed in the sarcolemma in heart from control mice, as shown by confocal immunofluorescence microscopy (Jungsuwadee et al., 2006). We examined the effect of DOX treatment on localization of Mrp1 and found that Mrp1 was colocalized with SDHB, a mitochondrial inner membrane marker. In saline-treated mice, there was little colocalization of the Mrp1 (green) and mitochondrial SDHB (red) signals (Fig. 1D). However, by 24 h after DOX treatment, Mrp1 protein expression in sarcolemma was retained and seemed to increase (Fig. 1F), whereas a significant amount of Mrp1 was colocalized with SDHB (Fig. 1H). Significant colocalization of Mrp1 with SDHB was also detected and seemed to have increased at 72 h after DOX treatment as more Mrp1 and SDHB were colocalized and the signals became yellow in the merged image (Fig. 1L).

To further examine these findings, the heart sections from mice killed 24 h after DOX or saline were labeled with immunogold for electron microscopy using anti-MRPr1 mAb. Electron-dense beads indicated positive staining for Mrp1 in cardiac mitochondria from DOX-treated mice (Fig. 2A). Quantitative analysis showed that the number of Mrp1-labeled beads in mitochondria was significantly increased approximately 2-fold in DOX- versus saline-treated mice (Fig.

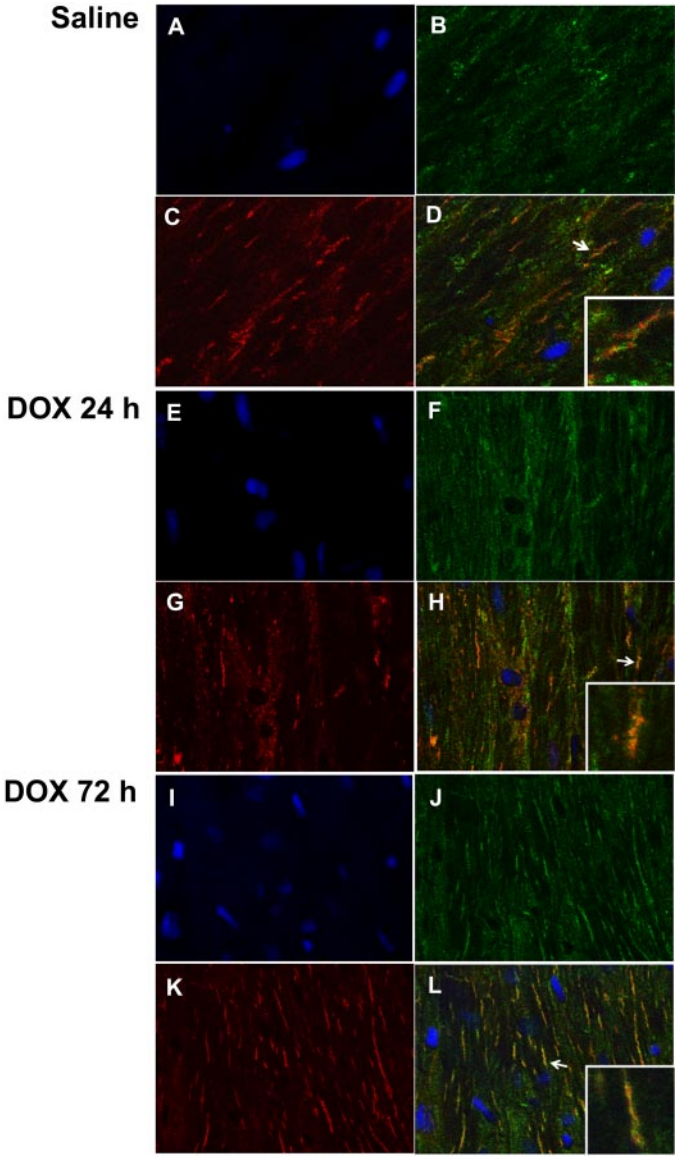

Fig. 1. Confocal immunofluorescent localization of Mrp1. Heart cryosections were stained for nuclei (blue), Mrp1 (green), and SDHB (red). A to D, a section from saline-treated mice stained and visualized for Mrp1 (B), SDHB (C), and merged (D). E to H, a section from DOX-treated mice taken at 24 h and stained for Mrp1 (F), SDHB (G), and merged (H); I to L, a section from DOX-treated mice taken at 72 h and stained for Mrp1 (J), SDHB (K), and merged (L) at 63×. Insets, magnified area indicated by arrows.

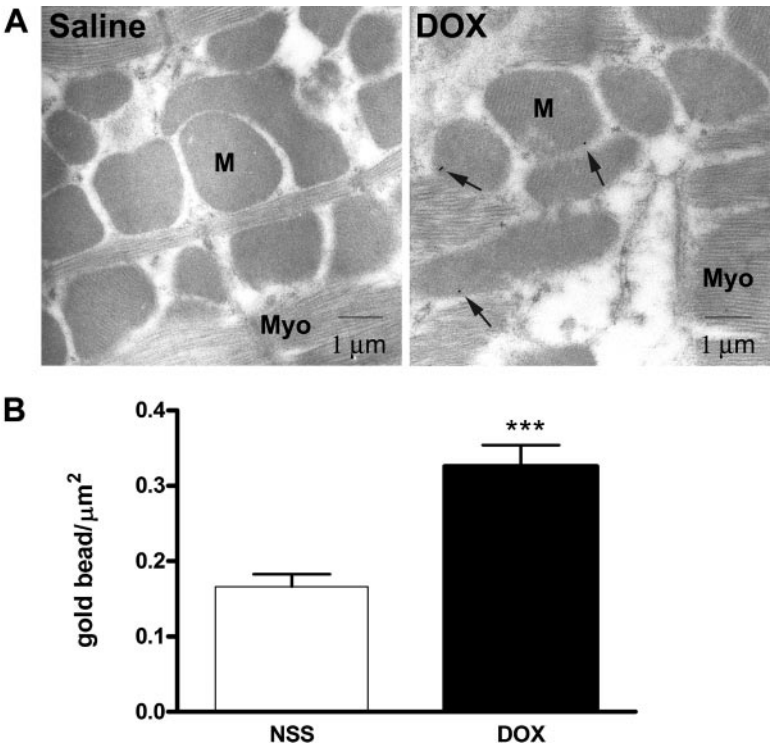

Fig. 2. Localization of Mrp1 in mitochondria by immunogold electron microscopy. A, representative cardiomyocytes from mice 24 h after treatment with saline or DOX. Arrows, electron-dense beads indicate positive staining for Mrp1 using anti-MRPr1 mAb. Cardiomyocytes from mice treated with DOX demonstrated labeling of Mrp1 in mitochondria (M). No significant labeling was found in myofilaments (Myo); magnification, 11,800×. B, quantitation of Mrp1-labeled beads in saline or DOX treatment groups. ***, $p < 0.001$ versus saline.

2B). These data clearly confirm the increased mitochondrial localization of Mrp1 after DOX treatment.

Identification of Mrp1 in SMP and Sarcolemma. We next characterized Mrp1 localization by subcellular fractionation and immunoblot analysis. SMP and sarcolemma were isolated from mouse hearts 24 h after DOX and Na^+/K^+-ATPase, a sarcolemma membrane marker, and activity and protein expression were determined by enzyme activity and immunoblot analysis, respectively. The enzyme assay indicated minimal (≤1 μmol/min/mg protein) Na^+/K^+-ATPase activity in SMP, whereas significant activity was detected in whole-heart homogenate; this activity was enriched 12-fold in sarcolemma relative to heart homogenate (Fig. 3A). Immunoblot analysis for Na^+/K^+-ATPase$_{\alpha 1}$ showed high expression in sarcolemma, whereas only trace amounts were detected in SMP (Fig. 3B). Mrp1 was highly enriched in sarcolemma but was also present in SMP, as determined by immunoblot analysis (Fig. 3B). To determine whether trace amounts of sarcolemma contamination of SMP, as indicated by Na^+/K^+-ATPase$_{\alpha 1}$, could be responsible for Mrp1 detected in SMP, we further purified SMP by centrifugation through 38% sucrose and analyzed for subcellular markers. MRPr1-positive bands remained clearly detected in such purified SMP membranes from DOX-treated mice relative to saline controls (Fig. 3C). SDHB (a mitochondria inner-membrane marker) was detected in SMP and whole-heart homogenate; however, no Na^+/K^+-ATPase$_{\alpha 1}$, LAMP2 (a lysosomal membrane marker), or GAPDH (a cytoplasmic marker) were detected in these purified SMP (Fig. 3C). Taken together, these data strongly support the presence of Mrp1 in mitochondria after DOX.

Mrp1 Transport Activity in SMP. We next examined the ATP-dependent transport activity of Mrp1 in membrane vesicles prepared from sarcolemma and SMP isolated 24 h after DOX. Significant Mrp1 transport activity for [^{3}H]$E_2$17G was demonstrated in SMP membrane vesicles (before further purification, as shown in Fig. 3B) that represented approximately one third that in sarcolemma vesicles (Fig. 3D); data in HEK_{Mrp1} membranes were included as a positive control. These results clearly demonstrate that after DOX treatment, ATP-dependent transport activity was localized both in mitochondria and in sarcolemma 24 h after DOX treatment. We also examined transport of LTC_4, using the further-purified SMP (as shown in Fig. 3C) in the presence and absence of the selective MRP1 inhibitor, MK571. ATP-dependent transport of [^{3}H]LTC_4 was significantly increased approximately two-fold 24 h after DOX treatment relative to saline controls, and this transport activity was significantly inhibited in the presence of MK571 (Fig. 3E).

Time Course of Mrp1 Transport Activity. As shown in Fig. 1, colocalization of Mrp1 with mitochondria proteins increased with time. To determine whether ATP-dependent transport activity of Mrp1 in SMP were also increased relative to increased colocalization of Mrp1 in mitochondria, transport in SMP isolated at different time points after DOX treatment was determined. These time course studies showed that ATP-dependent [^{3}H]$E_2$17G transport in SMP was significantly increased two-fold 24 h after DOX compared with saline controls, consistent with the 2-fold increase in LTC_4 transport (Fig. 3E) but was not sustained and was decreased at 48 and 72 h after DOX treatment (Fig. 3F).

Compartmentalization of Mrp1 Expression in Cardiac Tissue after DOX. To quantify the relative amounts of Mrp1 protein in sarcolemma versus SMP in mice treated with saline or DOX, we determined the Mrp1 expression levels by an immunoblot assay (Fig. 4). This was necessary because it is not possible to measure Mrp1-mediated transport activity in whole-heart homogenate. We first generated a standard curve for Mrp1 using membranes from HEK_{Mrp1} cells and quantitated Mrp1 band intensity in arbitrary units

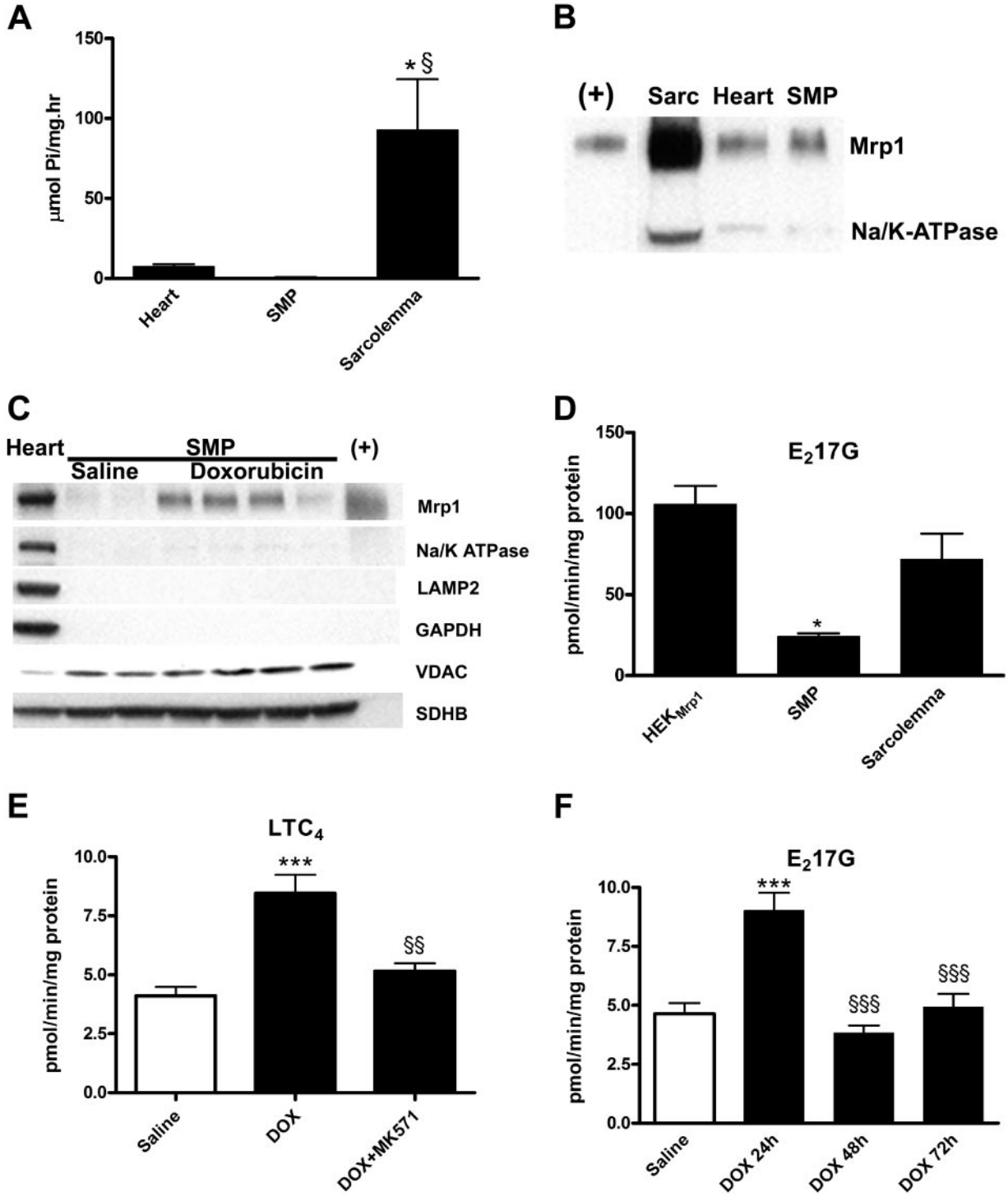

Fig. 3. Characterization of Na^+/K^+-ATPase and Mrp1 expression and activity in heart sarcolemma and SMP in mice 24 h after treatment with saline or DOX. A, Na^+/K^+-ATPase activity in whole-heart homogenate (Heart; 200 μg), SMP (200 μg), and sarcolemma (50 μg). Data represent mean ± S.E.M. of three independent experiments. *, $p < 0.05$ versus SMP; §, $p < 0.05$ versus heart. B, immunoblot analysis of Mrp1 in sarcolemma (Sarc; 25 μg), heart homogenate (Heart; 80 μg), and SMP (80 μg); HEK_{Mrp1} membranes (40 ng) were used as a positive control (+); note that this (+) lane was moved from lane 10 of this same gel. C, immunoblot analysis of Mrp1 and other subcellular protein markers in SMP (30 μg) prepared from C57BL/6 treated with saline or DOX and purified by discontinuous sucrose gradient; whole-heart homogenate (Heart) and HEK_{Mrp1} membranes (+) were used as controls. D, SMP and sarcolemma were assayed for [^{3}H]$E_2$17G transport. HEK_{Mrp1} membranes were used as a positive control. Data represent mean ± S.D. of triplicate determinations. An additional experiment was performed with similar results. *, $p < 0.05$ versus sarcolemma. E, ATP-dependent [^{3}H]LTC_4 transport in SMP purified by discontinuous sucrose gradient in saline- and DOX-treated mice in the presence and absence of MK571. ***, $p < 0.001$ versus saline; §§, $p < 0.01$ versus DOX. F, ATP-dependent [^{3}H]$E_2$17G transport in SMP in saline and DOX-treated mice 24, 48, and 72 h after DOX. Data represent mean ± S.E.M. of three independent experiments. ***, $p < 0.001$ versus saline; §§§, $p < 0.001$ versus DOX 24 h.

(Fig. 4A). We next obtained band densities of Mrp1 in heart homogenate (40 μg of protein) in saline-treated mice and at 12 and 24 h after DOX. Because the expression of Mrp1 at 12 and 24 h was similar in heart homogenate, we measured Mrp1 in sarcolemma and SMP at various protein concentrations in saline and DOX-treated mice at 24 h (Fig. 4B). Finally, we used the band densities obtained in sarcolemma (2 μg of protein) and SMP (40 μg of protein), and extrapolated the amounts of Mrp1 (in nanograms) from the Mrp1 standard curve (Fig. 4A) to estimate the amounts of Mrp1 in heart homogenate, sarcolemma, and SMP (Fig. 4C). Using this approach, after DOX treatment, Mrp1 expression increased 1.6-fold in whole-heart homogenate, whereas expression in sarcolemma increased approximately 2-fold, but increased 3-fold in SMP, indicating a concomitant increase in both cellular compartments.

Mrp1 Uptake of GS-HNE in SMP Vesicles. Because GSH conjugation of HNE in isolated liver mitochondria has been demonstrated (Chen et al., 2002), it is likely that a similar phenomenon could occur in the heart if GST were also expressed in cardiac mitochondria. As shown in Fig. 5A, GSTα expression was detected in mitochondria, although expression was not different between saline- and DOX-treated groups. Because GS-HNE is a substrate for MRP1 (Renes et al., 2000), we further examined whether SMP transported GS-HNE and whether this transport was increased after DOX treatment. ATP-dependent transport of [^{3}H]GS-HNE increased at least 2-fold at 24 h after DOX in a concentration-dependent manner (Fig. 5B). To determine whether the uptake of GS-HNE in SMP was osmotically sensitive, we incubated SMP with 3 μM [^{3}H]GS-HNE in the incubation buffer containing various sucrose concentrations. ATP-dependent uptake of 3 μM [^{3}H]GS-HNE increased as a linear function of the reciprocal of the sucrose concentrations, indicating that transport occurred into an osmotically sensitive space (Fig. 5C). In addition, preincubation of SMP with QCRL3, an MRP1-specific mAb, inhibited [^{3}H]GS-HNE uptake in SMP vesicles, indicating that GS-HNE uptake was Mrp1-specific (Fig. 5D). To ascertain further the role of Mrp1 in mediating ATP-dependent transport, we compared the SMP transport activity for [^{3}H]GS-HNE in saline and DOX-treated FVB mice and in DOX-treated Mrp1(−/−) mice 24 h after DOX treatment. ATP-dependent transport of [^{3}H]GS-HNE was increased 2-fold by DOX treatment in FVB mice and was negligible in Mrp1(−/−) mice treated with either saline or DOX (Fig. 5E).

DOX Increased Mrp1 Expression and Mrp1-HNE Adduction in SMP. In view of demonstrated mitochondrial HNE adducts after DOX treatment (Chaiswing et al., 2004) and based on data demonstrating a loss of ATP-dependent transport in SMP at 48 and 72 h after DOX (Fig. 3F), we postulated that adduction of mitochondrial Mrp1 with HNE could explain this loss of transport activity. We analyzed SMP from hearts of mice for HNE-Michael adducts and Mrp1 expression by immunoblots at 24, 48, and 72 h after DOX. As shown in Fig. 6A, HNE-adduction of a 190-kDa protein was increased at 48 and 72 h relative to 24 h. When the membrane was reprobed with anti-MRPr1 mAb, Mrp1 was detected in SMP at 24 h after treatment with DOX and increased further at 48 and 72 h (Fig. 6A). A similar experiment was carried out in FVB wild-type and

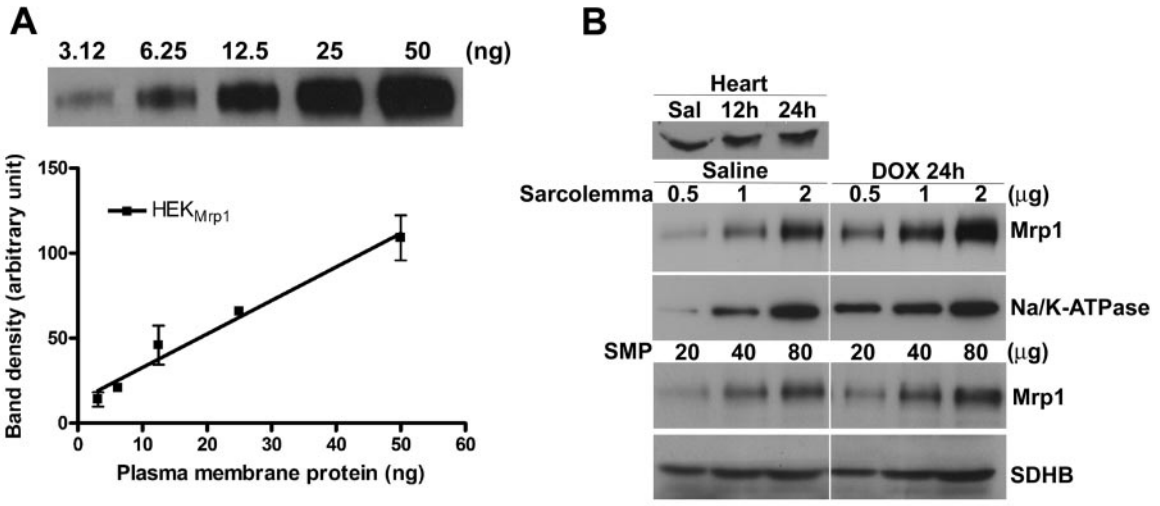

C

Treatment	Heart homogenate (40 μg)	SMP (40 μg)	Sarcolemma (2 μg)
	ng* Mrp1	ng* Mrp1	ng* Mrp1
Saline	3.62	2.15	13.6
DOX 24 h	5.65	6.29	31.6

Fig. 4. Compartmentalization of Mrp1 expression in cardiac tissue after DOX. A, a range of protein concentrations of HEK_{Mrp1} cells were fractionated on 4 to 12% gradient gel and nitrocellulose membranes probed for Mrp1. Band density was determined, expressed in arbitrary units, and plotted against the amount of membrane protein to obtain a standard curve. B, whole-heart homogenate (Heart), sarcolemma, and SMP purified by discontinuous sucrose gradient from C57BL/6 mice treated with saline or DOX (24 h) were probed for Mrp1; Na^+/K^+-$ATPase_{\alpha 1}$ (Na/K-ATPase) and SDHB were used as loading controls for sarcolemma and SMP, respectively. C, the amounts of Mrp1 (ng*, nanograms of HEK_{Mrp1} membrane protein) in heart homogenate, sarcolemma, and SMP were semiquantified based on band density and extrapolation from the Mrp1 standard curve (A).

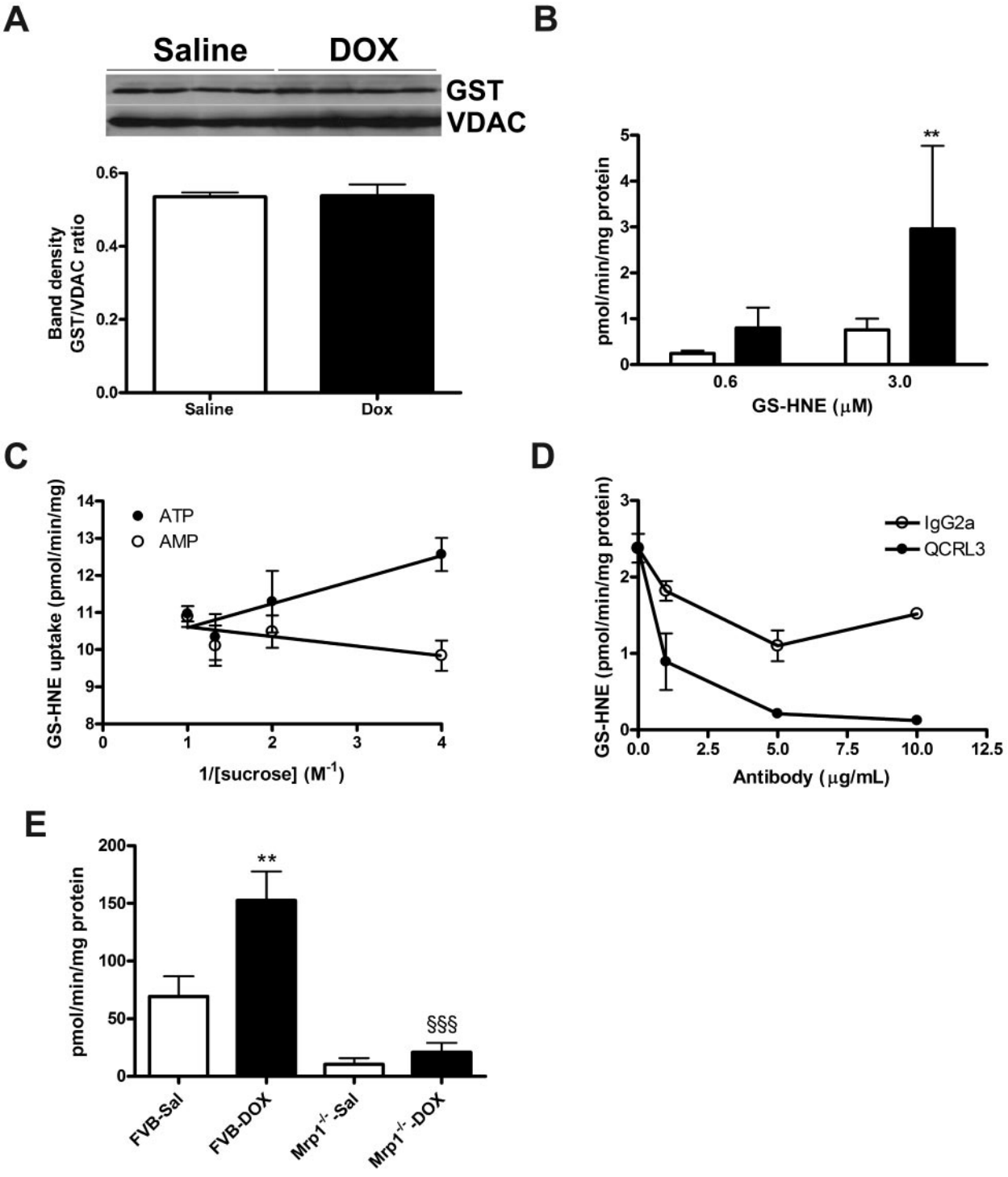

Fig. 5. GSTα expression and ATP-dependent transport in SMP after DOX. C57BL/6 mice were treated with DOX or saline and killed 24 h later. A, cardiac mitochondrial proteins (20 μg) were fractionated by 4 to 12% Tris-glycine gel, and the blot was probed for GSTα. The GSTα band densities were determined and normalized to VDAC, used as a loading control. The bar graph indicates the quantitation of GSTα after DOX relative to saline controls. Data represent mean of band densities ± S.D. (n = 4). B, cardiac SMP isolated from C57BL/6 mice treated with saline (□) or DOX 24 h (■) were incubated in buffer containing 0.6 or 3 μM [^{3}H]GS-HNE and ATP-dependent [^{3}H]GS-HNE transport determined. Data represent mean ± S.D. from triplicate determinations. **, $p < 0.01$. C, osmotic sensitivity of GS-HNE uptake. [^{3}H]GS-HNE (3 μM) uptake was measured in the presence of AMP (○) or ATP (●) in the presence of increasing sucrose concentrations (0.25–1 M) in the incubation buffer. Data represent mean ± S.E.M. of two independent experiments. D, SMP were preincubated on ice for 2 h in TS buffer containing IgG2a isotype control (○) or QCRL3 anti-MRP1 mAb (●) and [^{3}H]GS-HNE (3 μM) uptake determined. Data represent mean ± S.E.M. of two independent experiments. E, FVB and Mrp1(−/−) mice were treated with saline (Sal) or DOX (24 h) and ATP-dependent uptake of 3 μM [^{3}H]GS-HNE in SMP determined. Data represent mean ± S.D. from triplicate determinations. **, $p < 0.01$ compared with FVB-saline; §§§, $p < 0.001$ versus FVB-DOX.

Mrp1(−/−) mice to ensure that the 190-kDa protein represented Mrp1. DOX-treated FVB mice also showed increased Mrp1 expression in SMP, and an SMP protein with the same molecular weight as Mrp1 demonstrated marked HNE adduction. As expected, no Mrp1 was detected in either saline- or DOX-treated Mrp1(−/−) mice (Fig. 6B); importantly, the signal of HNE adducts at 190 kDa from Mrp1(−/−) mice was barely detectable relative to that in FVB wild-type mice treated with DOX (Fig. 6B). Finally, immunoprecipitation of Mrp1 in SMP from DOX-treated C57BL/6 mice followed by immunoblot analysis for HNE adducts confirmed increasing HNE adduction of Mrp1 after DOX (Fig. 6C). These results indicate that DOX increased Mrp1 expression in mitochondria; however, there was a concomitant increase in Mrp1-HNE adduction that correlated inversely with Mrp1 transport activity.

Mitochondria Dysfunction Caused by HNE. To determine the direct effect of HNE on the function of mitochondria, we investigated two parameters of mitochondrial function, ATP-dependent transport in SMP and mitochondrial respiration, in the presence and absence of HNE. SMP from mice treated with saline or DOX were incubated with either DMSO or 10 μM HNE before measuring transport activity. ATP-dependent [^{3}H]$E_2$17G transport was decreased by 74% in HNE-treated SMP compared with DMSO-treated controls. Similar experiments showed that ATP-dependent [^{3}H]LTC_4 transport was decreased by 50% in HNE-treated SMP compared with DMSO-treated controls (Fig. 7A). In the mitochondrial respiration assay, the respiratory control ratios in HNE-treated mitochondria were calculated and normalized to their DMSO controls. Respiration was significantly decreased in HNE-treated mitochondria (Fig. 7B). These data demonstrate the ability of HNE to cause mitochondrial dysfunction, by both inhibiting ATP-dependent transport activity in SMP vesicles and reducing mitochondrial respiration.

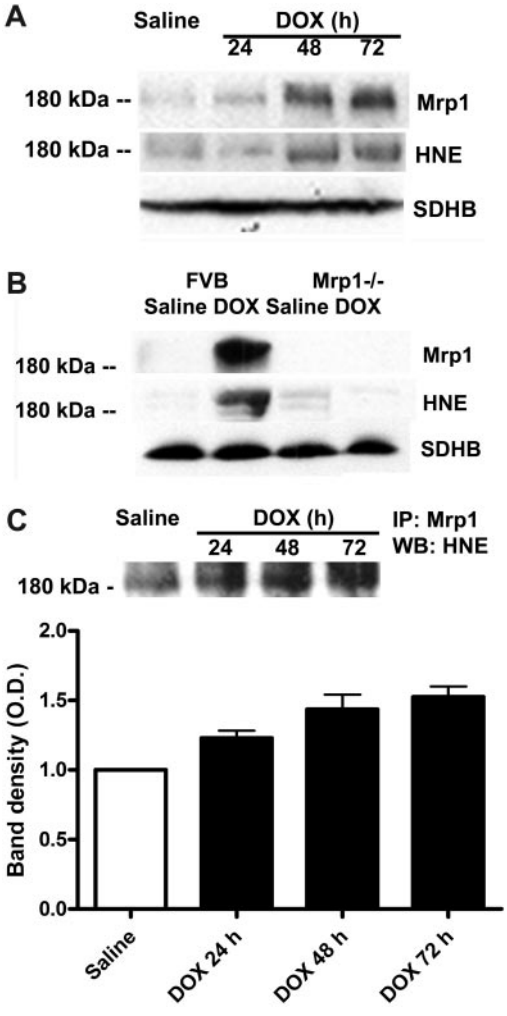

Fig. 6. Immunoblot analyses of Mrp1 and HNE-adducted protein in SMP. A, immunoblot analysis of SMP for Mrp1 and HNE-Michael adducts after saline or 24, 48, and 72 h after DOX. B, immunoblot analysis of SMP for Mrp1 and HNE-Michael adducts in FVB wild-type or Mrp1(−/−) mice treated with saline or 72 h after DOX. In A and B, the blot was first probed for HNE and then stripped and reprobed for Mrp1. C, immunoblot analysis of HNE in SMP after immunoprecipitation with anti-MRPr1 mAb. The bar graph indicates the -fold increase in HNE adducts after DOX relative to saline controls. Data represent the mean ± S.E.M. of band densities from duplicate determination from two independent experiments.

Discussion

Several lines of evidence support the finding of Mrp1 expression in mitochondria. First, confocal immunofluorescent microscopy confirmed constitutive Mrp1 expression in sarcolemma and found that Mrp1 also colocalized to mitochondria after DOX treatment. Second, immunogold electron micros-

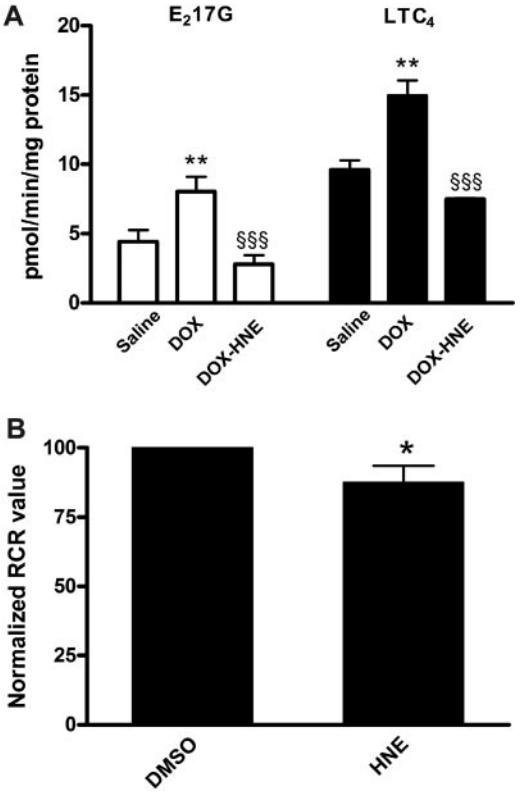

Fig. 7. Effects of HNE on ATP-dependent transport and mitochondrial respiration. A, SMP from saline and DOX-treated mice were incubated with DMSO or HNE (10 μM) in DMSO as indicated and ATP-dependent [^{3}H]$E_2$17G (□) or [^{3}H]LTC_4 (■) transport determined. Data represent the mean ± S.E.M. from three independent experiments. **, $p < 0.01$ versus saline; §§§, $p < 0.001$ versus DOX. B, cardiac mitochondria isolated 24 h after DOX were incubated with HNE (10 μM) or DMSO at 37°C for 20 min. Mitochondria respiration was performed, and respiratory control ratio values were calculated from the ratio between states 3 and 4 respiration and normalized to the DMSO control. *, $p < 0.05$ versus DMSO.

copy found a 2-fold increase in Mrp1 in mitochondria within 24 h after DOX. Third, subcellular fractionation of the heart identified Mrp1 in SMP and in sarcolemma at 24 h, based on both immunoblot analysis and ATP-dependent transport activity. The substantial ATP-dependent transport activity in SMP, together with the lack of detectable contamination with lysosomes (LAMP2), argues against contamination of SMP with inactivated Mrp1 destined for lysosomal degradation. That Mrp1 detected in SMP was not due to contamination with sarcolemma is supported by the very low level of Na^+/K^+-ATPase activity detected in SMP (i.e., ≤ 1 μmol/h/mg protein) (Fig. 3A). Given the 99 μmol/h/mg protein Na^+/K^+-ATPase activity detected in sarcolemma, this represents approximately 1% contamination of SMP by sarcolemma. Sarcolemma show 77 pmol/min/mg protein ATP-dependent transport of $E_2$17G (Fig. 3D); if such ATP-dependent transport in SMP were due to 1% sarcolemma contamination, it should not exceed 1 pmol/min/mg protein. Therefore, the ATP-dependent transport activity of 8 pmol/min/mg protein for $E_2$17G determined in SMP (DOX 24 h, Fig. 3F) indicates that the majority of this ATP-dependent transport activity is not due to contamination with sarcolemma. When SMP was further purified by centrifugation through a discontinuous sucrose gradient, Mrp1 expression and ATP-dependent LTC_4 transport were retained (Fig. 3, C and E, respectively). LTC_4 (100 nM) transport in sarcolemma vesicles is 63 pmol/min/mg (Jungsuwadee et al., 2006), whereas that in purified SMP was 8.5 pmol/min/mg protein (Fig. 3E), again reflecting approximately 13-fold greater transport activity in SMP than can be accounted for by 1% sarcolemma contamination.

Critical to the validity of these data are the specificity of the antibody to Mrp1. The anti-MRPr1 mAb, characterized by Hipfner et al. (1998) and Scheffer et al. (2000) is specific for the ^{238}GSDLWSLNKE^{247} epitope of MRP1 (Hipfner et al., 1998), a sequence that is poorly conserved in other family members of ABC transport proteins. This antibody was shown not to cross-react with MRP2, MRP3, MRP5, MDR1, or BCRP (Scheffer et al., 2000), and we have not found it to cross-react with other proteins in Mrp1(−/−) mice by immunoblotting (Fig. 6B) or confocal immunofluorescence (data not shown). These data, together with the ability of MK571 and QCRL3 mAb to inhibit LTC_4 and GS-HNE transport, support the conclusion that ATP-dependent transport activity in SMP is Mrp1-mediated. Taken together, these data provide compelling evidence for the mitochondrial localization of functional Mrp1 after DOX treatment. Whereas specific transport activity (in picomoles per minutes per milligram of protein) is 3- to 4-fold higher in sarcolemma than in SMP, it can be calculated that most of the total Mrp1 activity in heart after DOX treatment is associated with mitochondria, because mitochondrial protein represents approximately 40% of the noncollagenous protein of cardiac tissue (Idell-Wenger et al., 1978), whereas sarcolemma represents approximately 2% of the protein (data not shown).

A discrepancy between localization of Mrp1 in mitochondria that was further increased at 48 and 72 h by immunoblot analysis, and ATP-dependent transport activity in SMP that was maximal at 24 h, was shown to be due to HNE adduction of Mrp1 at the later times. We have shown that the addition of HNE to sarcolemma (Jungsuwadee et al., 2006) and SMP (Fig. 6A) inhibits ATP-dependent transport (Fig. 7A), consistent with apparent loss of transport activity with increased HNE adduction of Mrp1. We also demonstrated the presence of GSTα in mitochondria (Fig. 5A). Although glutathione transferases have been shown to be up-regulated in cardiomyocytes after exposure to DOX (Paranka and Dorr, 1994), and oxidative stress increases the expression of mitochondrial glutathione transferase A4-4 (Raza et al., 2002), we did not detect a difference in GSTα expression in mitochondria between saline and DOX-treated mice. We also detected the presence of GS-HNE in mitochondria from DOX-treated mice (data not shown). Although conjugation with GSH significantly decreases HNE reactivity, GS-HNE retains some toxicity (Renes et al., 2000) and is postulated to feedback-inhibit further GST-mediated conjugation of HNE with GSH (Hubatsch et al., 1998). Given the presence of GSTα in mitochondria, the formation of GS-HNE in mitochondria (Hill et al., 2009), and the toxicity of GS-HNE, a mechanism for removal of GS-HNE from mitochondria would seem to be a useful protective mechanism. It is plausible, therefore, that mitochondrial Mrp1 serves to efflux GS-HNE, followed by its efflux across the sarcolemma to protect the cardiomyocyte. In the case of failure to conjugate and efflux HNE, the accumulation of HNE protein adducts can inactivate Mrp1. Whether the HNE adduction modifies the tertiary structure of Mrp1 and whether there is a 1:1 correlation between the amount of HNE adduction of Mrp1 and its decreased transport activity is unclear. Nevertheless, HNE adduction of Mrp1 would prevent the Mrp1 from transporting substrates out of mitochondria, thereby probably further increasing oxidative damage.

The semiquantitation of Mrp1 in homogenate, sarcolemma, and SMP indicates that the total amount of Mrp1 in the heart increased by 24 h and suggests an independent localization of Mrp1 to these distinct compartments and not a translocation from the sarcolemma to the mitochondria. Further studies are needed to characterize the mechanism by which Mrp1 localizes to mitochondria. Mitochondrial Mrp1 does not seem to be glycosylated differently relative to sarcolemma or HEK_{Mrp1} membranes, based on its apparent molecular weight. In addition, Mrp1 does not have a mitochondrial localization sequence as predicted by WoLF PSORT (available at http://wolfpsort.org/) (Horton et al., 2007). However, a majority of mitochondrial proteins, including ABCB6, an ATP-dependent porphyrin transporter recently demonstrated to be located in the outer mitochondrial membrane (Krishnamurthy et al., 2006; Paterson et al., 2007) and the plasma membrane (Paterson et al., 2007), lack such a canonical sequence (Krishnamurthy et al., 2006). The presence of ABCB6 in plasma membrane and mitochondrial membrane (Krishnamurthy et al., 2006; Paterson et al., 2007) and in intracellular vesicular membranes (Jalil et al., 2008) and the presence of MRP1 in subcellular compartments (Rajagopal and Simon, 2003) provide evidence that ABC transporters can be present in multiple cellular compartments. Avadhani and colleagues have demonstrated that some cytochrome P450 isoforms, localized predominantly in the endoplasmic reticulum of liver, are also present in mitochondria, the result of revelation of cryptic mitochondrial targeting sequences (Robin et al., 2002), including those induced by oxidative stress. Because both VDAC and SDHB were detected in purified SMP, we cannot at present specify whether Mrp1 is localized to the outer or inner mitochondrial membrane (Fig. 3C). Likewise, although we postulate that Mrp1 functions to efflux substrates from the mitochondria,

we cannot rule out the transport of substrate into mitochondria.

In summary, the present studies have demonstrated that functional Mrp1 is localized in mitochondria within 24 h after treatment with DOX, and suggest that this represents an early adaptive response to DOX-induced oxidative stress. However, Mrp1 activity was decreased with time, most likely as a result of adduction with HNE. Taken together, our data suggest that the up-regulation of Mrp1 in heart and cardiac mitochondria after DOX treatment represents a physiological function of Mrp1 in protecting the heart by mediating the efflux of toxic products of oxidative stress. Hence, accumulation of toxic oxidative products such as HNE in mitochondria, resulting in inhibition of mitochondrial respiration, together with HNE-adduction and inhibition of Mrp1, may contribute to the cause of DOX-induced cardiomyopathy.

Acknowledgments

The pCEBV7-Mrp1 was generously provided by Dr. Roger G. Deeley.

References

Alin P, Danielson UH, and Mannervik B (1985) 4-Hydroxyalk-2-enals are substrates for glutathione transferase. *FEBS Lett* **179:**267–270.
Chabner BA, Ryan DP, Paz-Ares L, Garcia-Carbonero R, and Calabresi P (2001) Antineoplastic Agents, in *Goodman & Gilman's The Pharmacological Basis of Therapeutics* (Hardman JG, Limbird LE eds) pp 1389–1495, McGraw-Hill Medical Publishing Division, New York.
Chaiswing L, Cole MP, St Clair DK, Ittarat W, Szweda LI, and Oberley TD (2004) Oxidative damage precedes nitrative damage in Adriamycin-induced cardiac mitochondrial injury. *Toxicol Pathol* **32:**536–547.
Chen J, Schenker S, and Henderson GI (2002) 4-hydroxynonenal detoxification by mitochondrial glutathione S-transferase is compromised by short-term ethanol consumption in rats. *Alcohol Clin Exp Res* **26:**1252–1258.
Cole SP, Bhardwaj G, Gerlach JH, Mackie JE, Grant CE, Almquist KC, Stewart AJ, Kurz EU, Duncan AM, and Deeley RG (1992) Overexpression of a transporter gene in a multidrug-resistant human lung cancer cell line. *Science* **258:**1650–1654.
Deeley RG and Cole SP (2006) Substrate recognition and transport by multidrug resistance protein 1 (ABCC1). *FEBS Lett* **580:**1103–1111.
Flens MJ, Zaman GJ, van der Valk P, Izquierdo MA, Schroeijers AB, Scheffer GL, van der Groep P, de Haas M, Meijer CJ, and Scheper RJ (1996) Tissue distribution of the multidrug resistance protein. *Am J Pathol* **148:**1237–1247.
Freireich EJ, Gehan EA, Rall DP, Schmidt LH, and Skipper HE (1966) Quantitative comparison of toxicity of anticancer agents in mouse, rat, hamster, dog, monkey, and man. *Cancer Chemother Rep* **50:**219–244.
Gille L and Nohl H (1997) Analyses of the molecular mechanism of Adriamycin-induced cardiotoxicity. *Free Radic Biol Med* **23:**775–782.
Hansen JM, Go YM, and Jones DP (2006) Nuclear and mitochondrial compartmentation of oxidative stress and redox signaling. *Annu Rev Pharmacol Toxicol* **46:**215–234.
Hill BG, Awe SO, Vladykovskaya E, Ahmed Y, Liu SQ, Bhatnagar A, and Srivastava S (2009) Myocardial ischaemia inhibits mitochondrial metabolism of 4-hydroxy-trans-2-nonenal. *Biochem J* **417:**513–524.
Hipfner DR, Gao M, Scheffer G, Scheper RJ, Deeley RG, and Cole SP (1998) Epitope mapping of monoclonal antibodies specific for the 190-kDa multidrug resistance protein (MRP). *Br J Cancer* **78:**1134–1140.
Horton P, Park KJ, Obayashi T, Fujita N, Harada H, Adams-Collier CJ, and Nakai K (2007) WoLF PSORT: protein localization predictor. *Nucleic Acids Res* **35:**W585–W587.
Hubatsch I, Ridderström M, and Mannervik B (1998) Human glutathione transferase A4–4: an alpha class enzyme with high catalytic efficiency in the conjugation of 4-hydroxynonenal and other genotoxic products of lipid peroxidation. *Biochem J* **330:**175–179.
Idell-Wenger JA, Grotyohann LW, and Neely JR (1978) Coenzyme A and carnitine distribution in normal and ischemic hearts. *J Biol Chem* **253:**4310–4318.
Ishikawa T, Esterbauer H, and Sies H (1986) Role of cardiac glutathione transferase and of the glutathione S-conjugate export system in biotransformation of 4-hydroxynonenal in the heart. *J Biol Chem* **261:**1576–1581.
Jain KK and Fischer B (1989) *Oxygen in Physiology and Medicine*. Charles C Thomas, Springfield, IL.
Jalil YA, Ritz V, Jakimenko A, Schmitz-Salue C, Siebert H, Awuah D, Kotthaus A, Kietzmann T, Ziemann C, and Hirsch-Ernst KI (2008) Vesicular localization of the rat ATP-binding cassette half-transporter rAbcb6. *Am J Physiol Cell Physiol* **294:**C579–C590.
Jungsuwadee P, Cole MP, Sultana R, Joshi G, Tangpong J, Butterfield DA, St Clair DK, and Vore M (2006) Increase in Mrp1 expression and 4-hydroxy-2-nonenal adduction in heart tissue of Adriamycin-treated C57BL/6 mice. *Mol Cancer Ther* **5:**2851–2860.
Krishnamurthy PC, Du G, Fukuda Y, Sun D, Sampath J, Mercer KE, Wang J, Sosa-Pineda B, Murti KG, and Schuetz JD (2006) Identification of a mammalian mitochondrial porphyrin transporter. *Nature* **443:**586–589.
Linnane AW and Ziegler DM (1958) Studies on the mechanism of oxidative phosphorylation. V. The phosphorylating properties of the electron transport particle. *Biochim Biophys Acta* **29:**630–638.
Mela-Riker LM and Bukoski RD (1985) Regulation of mitochondrial activity in cardiac cells. *Annu Rev Physiol* **47:**645–663.
Oberley TD (2002) Ultrastructural localization and relative quantification of 4-hydroxynonenal-modified proteins in tissues and cell compartments. *Methods Enzymol* **352:**373–377.
Paranka NS and Dorr RT (1994) Effect of doxorubicin on glutathione and glutathione-dependent enzymes in cultured rat heart cells. *Anticancer Res* **14:**2047–2052.
Paterson JK, Shukla S, Black CM, Tachiwada T, Garfield S, Wincovitch S, Ernst DN, Agadir A, Li X, Ambudkar SV, et al. (2007) Human ABCB6 localizes to both the outer mitochondrial membrane and the plasma membrane. *Biochemistry* **46:**9443–9452.
Piscitelli SC, Rodvold KA, Rushing DA, and Tewksbury DA (1993) Pharmacokinetics and pharmacodynamics of doxorubicin in patients with small cell lung cancer. *Clin Pharmacol Ther* **53:**555–561.
Rajagopal A and Simon SM (2003) Subcellular localization and activity of multidrug resistance proteins. *Mol Biol Cell* **14:**3389–3399.
Raza H, Robin MA, Fang JK, and Avadhani NG (2002) Multiple isoforms of mitochondrial glutathione S-transferases and their differential induction under oxidative stress. *Biochem J* **366:**45–55.
Renes J, de Vries EE, Hooiveld GJ, Krikken I, Jansen PL, and Müller M (2000) Multidrug resistance protein MRP1 protects against the toxicity of the major lipid peroxidation product 4-hydroxynonenal. *Biochem J* **350:**555–561.
Robin MA, Anandatheerthavarada HK, Biswas G, Sepuri NB, Gordon DM, Pain D, and Avadhani NG (2002) Bimodal targeting of microsomal CYP2E1 to mitochondria through activation of an N-terminal chimeric signal by cAMP-mediated phosphorylation. *J Biol Chem* **277:**40583–40593.
Scheffer GL, Kool M, Heijn M, de Haas M, Pijnenborg AC, Wijnholds J, van Helvoort A, de Jong MC, Hooijberg JH, Mol CA, et al. (2000) Specific detection of multidrug resistance proteins MRP1, MRP2, MRP3, MRP5, and MDR3 P-glycoprotein with a panel of monoclonal antibodies. *Cancer Res* **60:**5269–5277.
Singal PK and Iliskovic N (1998) Doxorubicin-induced cardiomyopathy. *N Engl J Med* **339:**900–905.
Srivastava S, Chandra A, Wang LF, Seifert WE Jr, DaGue BB, Ansari NH, Srivastava SK, and Bhatnagar A (1998) Metabolism of the lipid peroxidation product, 4-hydroxy-trans-2-nonenal, in isolated perfused rat heart. *J Biol Chem* **273:**10893–10900.
Zhou S, Starkov A, Froberg MK, Leino RL, and Wallace KB (2001) Cumulative and irreversible cardiac mitochondrial dysfunction induced by doxorubicin. *Cancer Res* **61:**771–777.

Address correspondence to: Dr. Mary Vore, Graduate Center for Toxicology, 1095 VA Drive, 306 Health Sciences Research Building, Lexington, KY 40536-0305. E-mail: maryv@uky.edu